Journal of Power Sources 225 (2013) 108–112

Contents lists available at SciVerse ScienceDirect

Journal of Power Sources

journal homepage: www.elsevier.com/locate/jpowsour

Short communication

Synthesis of SnO_2 nano hollow spheres and their size effects in lithium ion battery anode application

Won-Sik Kim, Yoon Hwa, Jeong-Hoon Jeun, Hun-Joon Sohn, Seong-Hyeon Hong*

Department of Materials Science and Engineering, Research Institute of Advanced Materials (RIAM), Seoul National University, Seoul 151-744, Republic of Korea

HIGHLIGHTS

- Size controlled SnO_2 hollow spheres are synthesized for an anode of LIB.
- The size of hollow sphere strongly affects the electrochemical properties.
- The reversible capacity of 25 nm hollow sphere is ~750 mA g^{-1} after 50 cycles.

GRAPHICAL ABSTRACT

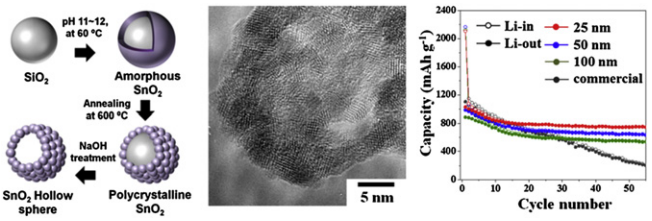

ARTICLE INFO

Article history:
Received 21 June 2012
Received in revised form
15 September 2012
Accepted 12 October 2012
Available online 22 October 2012

Keywords:
Tin oxide
Hollow sphere
Size-control
Lithium ion battery

ABSTRACT

Nano-sized SnO_2 hollow spheres are facilely synthesized by sol–gel method using the SiO_2 nanospheres as sacrificed templates, and their electrochemical properties are investigated as an anode application for lithium ion battery (LIB). The size of the hollow spheres is controlled by using different-sized templates. As-coated SnO_2 shell is almost amorphous and transformed into a rutile phase after annealing at 600 °C. The size of the SnO_2 hollow spheres ranges from 25 to 100 nm. The shell thickness is almost constant (~5 nm) irrespective of the size of the hollow spheres. The hollow spheres showed the size dependent electrochemical properties, and the smallest SnO_2 (25 nm) hollow sphere exhibited a high reversible capacity of 750 mAh g^{-1} as well as excellent cyclability.

1. Introduction

The demand for high energy and power density lithium ion batteries (LIBs) has increased for use in hybrid electric vehicles (HEVs) as well as in light-weight and portable electronic devices [1]. In commercial LIBs, graphite-based materials are widely used as anodes, but the theoretical capacity is only 372 mAh g^{-1} [2]. Therefore, intensive researches have focused on high capacity electrode materials such as Si, Ge, Sn, SnO_2 [3,4]. Among various candidates, SnO_2 is attractive as a promising anode material due to its high capacity and low reactivity with electrolytes [5]. However, a large and uneven volume change of 300% occurs upon lithium insertion/extraction, which causes a pulverization and electrical connectivity loss. As a result, the SnO_2 electrode shows a rapid capacity fading.

To mitigate this problem, various nanostructures have been applied to the LIB anodes [6,7]. Among them, hollow spheres are the most promising structure for the anode electrode of LIBs due to a low density, high surface to volume ratio, and structural stability [6]. Recently, the electrochemical properties of SnO_2-based hollow structures have been intensively investigated, and these structures showed an enhanced cycling performance compared to the solid SnO_2 nanoparticles [8–10]. However, most of the studies have focused on the fabrication of unique nanostructures, and their size was limited to 100–200 nm. While the size of hollow spheres appears to be a crucial factor, the synthesis of size-controlled hollow spheres and the size dependence of the electrochemical properties have not been explored.

* Corresponding author. Tel.: +82 2 880 6273; fax: +82 2 885 1748.
E-mail address: shhong@snu.ac.kr (S.-H. Hong).

0378-7753/$ – see front matter © 2012 Elsevier B.V. All rights reserved.
http://dx.doi.org/10.1016/j.jpowsour.2012.10.030

In this study, the size effect of SnO_2 hollow spheres is investigated for LIB anode application. The nano-sized SnO_2 hollow spheres are fabricated by SiO_2 template-based synthesis and the size of the hollow spheres is controlled by using different-sized templates.

2. Experimental

SiO_2 colloids with different sizes were prepared by the modified Stöbber method [11]. The size of silica nanoparticles was controlled by the amount of catalysts (28% ammonium hydroxide). The contents of reactants, solvent, catalyst, and pH value are shown in Table S1 (see Electronic Supplementary Material). For synthesis of SiO_2 colloid, 75 mL methanol (Carlo Erba Reagents), 10 mL deionized water, and required amount of ammonium hydroxide (Samchun Chemical) were first mixed, and then, 2 mL of tetraethylorthosilicate (TEOS, 98+%, Sigma Aldrich) was added. The reaction was conducted at room temperature for 2 h. The prepared SiO_2 colloid solution was repeatedly washed with deionized water until pH reached about 8. The final volume of each SiO_2 colloid solution was 50 mL. The SnO_2 hollow spheres were fabricated by using the prepared SiO_2 colloid solutions. In a typical experiment (25 nm SnO_2 hollow sphere), 0.8 g of potassium stannate trihydrate ($K_2SnO_3 \cdot 3H_2O$, Sigma Aldrich) was dissolved in 45 mL deionized water and 5 mL of prepared SiO_2 colloid solution was added. And then, 25 mL of absolute ethanol was added to the above solution. The solution was heated to 60 °C for 1 h with a mild stirring. The shell coating temperature was varied from 40 to 100 °C, but no specific change of SnO_2 shell formation was observed. The white product was collected by centrifuge and washed three times with deionized water, dried at 100 °C, and annealed at 600 °C for 1 h. The annealed powder was treated with 2 M NaOH solution at 50 °C for 1 h. Subsequently, the SnO_2 hollow sphere was obtained.

For electrochemical measurements, the test electrodes consisted of active powder material (0.2 g), carbon black (Ketchen Black, 0.06 g) as a conducting agent and poly amide imide (PAI, 0.03 g) dissolved in N-methyl pyrrolidinone (NMP) at 60 °C as a binder. Each component was well mixed to form a slurry using a magnetic stirrer. The slurry was coated on a copper foil substrate, pressed, and dried at 200 °C for 4 h under a vacuum. A coin-type electrochemical cell was used with Li foil as the counter and reference electrodes, and 1 M $LiPF_6$ in ethylene carbonate (EC)/diethylene carbonate (DEC) (5:5 (v/v), PANAX) was used as the electrolyte. The amount of active material loading on each copper foil was 1 mg and the mass of Li foil was 70 mg. The cell assembly and all electrochemical tests were carried out in an Ar-filled glove box. The cycling experiments were galvanostatically performed using a Maccor automated tester at a constant current density of 100 mA g^{-1} for the active material within a voltage range between 0.0 and 2.5 V (vs. Li/Li+). The rate capability test was conducted in the following sequence of current density: 100, 300, 500, 1000, 1500, and 100 mA g^{-1}. For reference, commercial SnO_2 nanopowder (<100 nm, Sigma Aldrich) was also examined.

3. Results and discussion

The low magnification TEM image (Fig. 1a) reveals the core–shell structure with bright center (SiO_2 template) and dark shell (SnO_2 layer). The shell thickness is quite uniform. The SnO_2 layer is almost amorphous, but nanocrystallites are occasionally observed (Fig. 1b). After annealing at 600 °C and removing SiO_2 in NaOH, the SnO_2 hollow structure is maintained (Fig. 1c). The average size of the SnO_2 hollow sphere was about 25 nm and the individual hollow sphere was agglomerated. The high magnification TEM image reveals that the hollow spheres are composed of interconnected nanocrystallites of ~3 nm size (Fig. 1d). The lattice fringes are clearly discerned and the interplanar spacings are determined to be 0.335 and 0.264 nm, which are in good agreement with the (110) and (101) planes of SnO_2, respectively. The shell thickness was less than 5 nm, which indicates that the hollow sphere shell consists of a maximum of one or two nanocrystallites. The selected area electron diffraction (SAED) patterns of SiO_2–SnO_2 core-shells (upper) and SnO_2 hollow spheres (bottom) are shown in Fig. 1e. In SiO_2–SnO_2 core-shells, a clear diffraction pattern is not observed, whereas the ring patterns are evident in the SnO_2 hollow spheres, which are completely indexed to rutile SnO_2. The crystal structure of the samples is further investigated by X-ray diffraction (XRD) (Fig. 1f). The diffraction peaks for as-coated SiO_2–SnO_2 core-shells are broad with a very weak intensity because the SnO_2 shells are not completely crystallized during the coating process. After annealing at 600 °C and removing SiO_2, the SnO_2 hollow spheres are crystallized into a single phase rutile SnO_2. All the peaks are broadened due to the nanocrystalline nature of the SnO_2 particles. This result agrees well with the TEM image. To determine the specific surface area, Brunauer–Emmett–Teller (BET) nitrogen absorption/desorption analysis is performed. The BET surface area of annealed SiO_2–SnO_2 core-shells is 41.0 m^2 g^{-1} and that of SnO_2 hollow spheres is around 117.9 m^2 g^{-1}. This increase is attributed to the hollow nature and nanoporous shell. The synthesis temperature of the SnO_2 shell layer is varied from 40 to 100 °C, but no specific morphology change is observed (Fig. S1, see Electronic Supplementary Material). Hydrothermal method is commonly employed for SnO_2 coating, which requires a relatively high temperature (>160 °C) and a long processing time [12]. The Sn precursor ($K_2SnO_3 \cdot 3H_2O$) and solvent (ethanol–water) adopted in this study are similar to those used in the hydrothermal process, but the nanosized SnO_2 coating is successfully synthesized at a low temperature for a short time.

The size of the hollow spheres is simply controlled by using different-sized SiO_2 templates, and the shell thickness is fixed at about 5 nm (Fig. 2). The larger sized SnO_2 hollow spheres require a small amount of SnO_2 precursor to achieve the constant shell thickness due to the decrease of surface area, i.e. the amount of $K_2SnO_3 \cdot 3H_2O$ is reduced (Table S2, see Electronic Supplementary Material). Three kinds of hollow SnO_2 spheres are fabricated in this study, and their average sizes are 25, 54, and 103 nm. Irrespective of the size, the hollow spheres are composed of interconnected nanoparticles of about 3 nm, and the SAED patterns confirmed the formation of rutile SnO_2 (Fig. S2, see Electronic Supplementary Material). For convenience, each sample is named the 25, 50, and 100 nm-sized SnO_2 hollow spheres.

The discharge/charge voltage profile of the 25 nm sized SnO_2 hollow sphere electrode is shown in Fig. 3a, and the shape of the voltage profile is similar to that of the typical SnO_2 [6,8,13]. The initial discharge and charge capacities are 2105 and 1029 mAh g^{-1}, respectively, which are higher than the theoretical values. The higher discharge capacity is due to the formation of Li_2O and solid electrolyte interphase (SEI) as well as additional reaction from the conducting agent. The higher charge capacity is attributed to the reversible polymerization of electrolyte [14,15]. The SnO_2 hollow spheres of the other sizes show similar voltage profiles (Fig. S3, see Electronic Supplementary Material). The low 1st cycle efficiency (about 48.9%) might be caused by the irreversible reduction of SnO_2 to Sn and the formation of Li_2O and SEI on the surface of the active material [5], which is expected to be improved by the addition of conducting materials (CNT, graphene) or transition metal oxides [16,17]. The rate capability test of the SnO_2 (25 nm) electrode (Fig. 3b) shows that the reversible capacity at a current density of 200 mA g^{-1} is about 700 mAh g^{-1} and it is about 530 mAh g^{-1} at 500 mA g^{-1}. This good rate capability is due to the nano-sized SnO_2

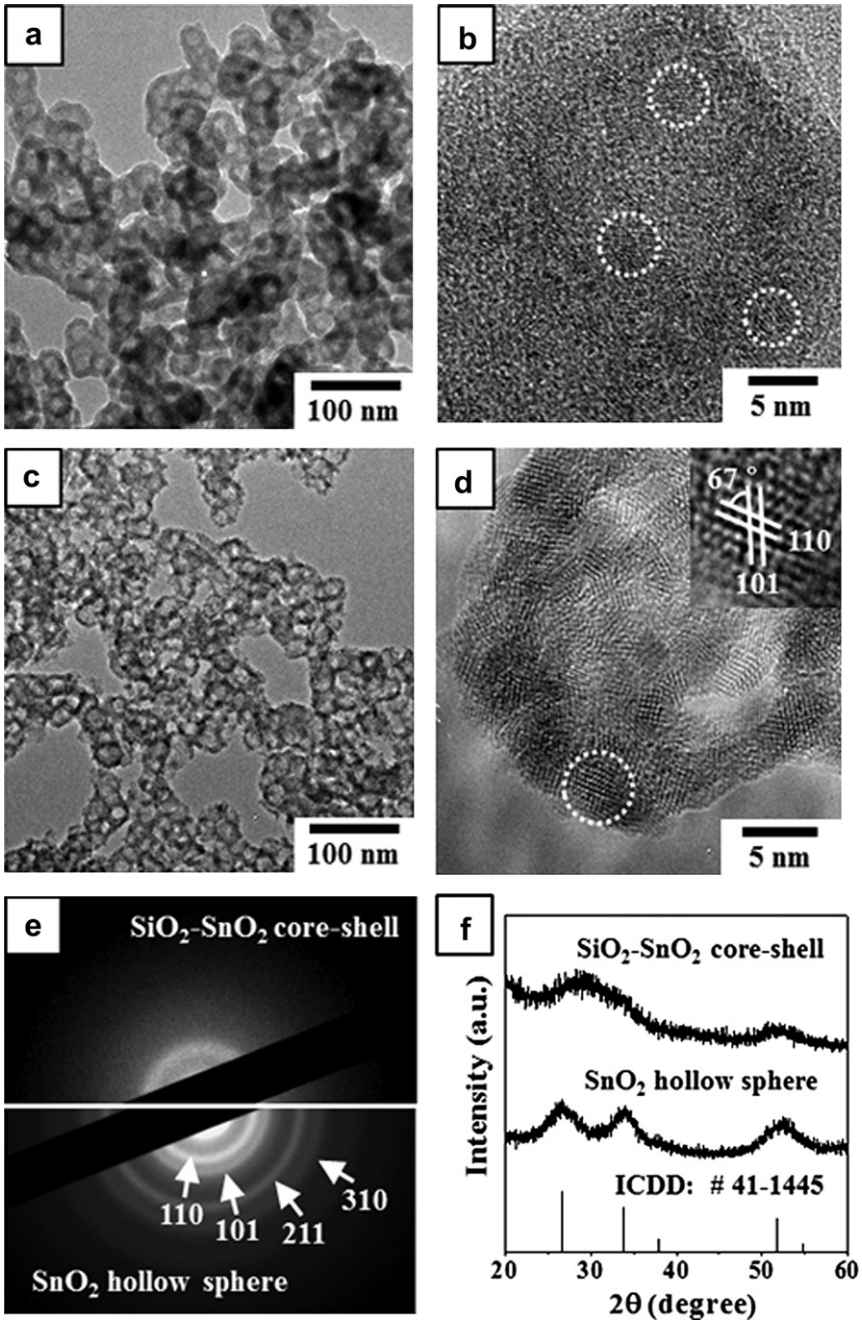

Fig. 1. (a) Low and (b) high magnification TEM images of as-coated SiO_2–SnO_2 core-shells; (c, d) 25 nm sized SnO_2 hollow spheres after annealing and removal of SiO_2; (e) SAED patterns of as-coated SnO_2–SiO_2 core-shells (upper) and SnO_2 hollow spheres (bottom); (f) XRD patterns of SiO_2–SnO_2 core-shells and SnO_2 hollow spheres.

hollow sphere and thin shell thickness. To demonstrate the size effects, the cyclability of each hollow SnO_2 is compared at a current density of 100 mA g^{-1} (Fig. 3c). All samples show good cyclability, but the reversible capacity of each electrode differs. The capacity is strongly dependent on the hollow size and increases with a decrease in the size of the hollow sphere. The capacity of the 100 nm sized SnO_2 hollow sphere is 547 mAh g^{-1} after 50 cycles, which is close to the previous result [13]. As the size of the SnO_2 hollow spheres is reduced, the electrodes show higher reversible capacities. The reversible capacity of the SnO_2 (25 nm) electrode is about 750 mAh g^{-1} after 50 cycles and this value is close to the theoretical capacity of SnO_2. To investigate the effect of the hollow structure on the electrochemical properties, the result of cycle test for the commercial SnO_2 nanopowder (9.55 m^2 g^{-1} of BET surface area) is included. The SnO_2 hollow sphere electrode shows better electrochemical properties than the SnO_2 nanopowder electrode. The cyclic capacity of the nanopowder continuously decreased, and the capacity was only 250 mAh g^{-1} after 50 cycles. After 50 cycles, the reversible capacity of the SnO_2 nanopowder is only 33% of the theoretical value. It is reported that the nanocrystalline CdS in spherical shell geometry is capable of withstanding extreme stresses [18], and the maximum tensile stress in a hollow Si sphere is ~5 times lower than that in a solid sphere with an equal volume of Si during lithiation [19]. The larger size SnO_2 hollow sphere is more fragile and it is inferred that the smaller sized hollow sphere is mechanically strong and more effectively endures the large

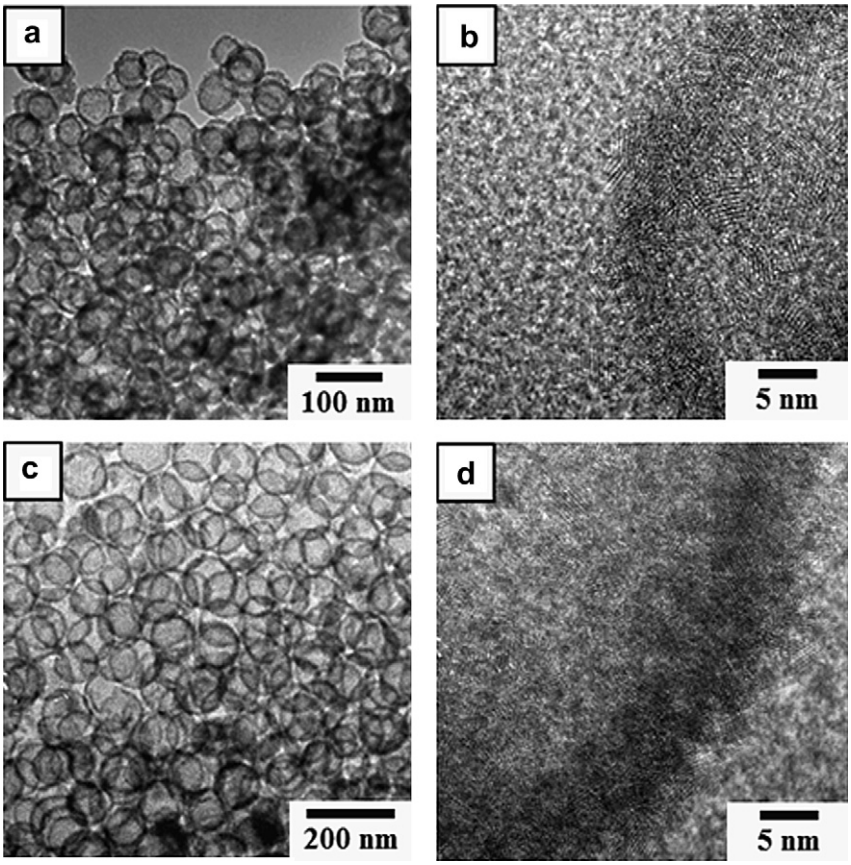

Fig. 2. TEM images of size controlled SnO_2 hollow spheres: (a, b) 50 nm; (c, d) 100 nm.

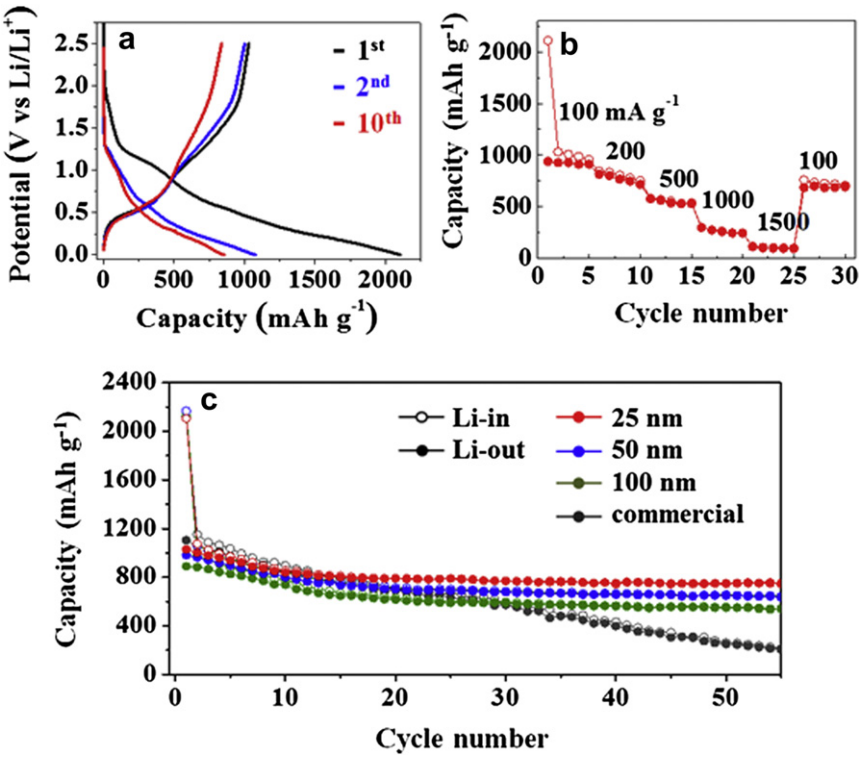

Fig. 3. (a) Charge/discharge voltage profile of 25 nm sized SnO_2 hollow sphere between 0.01 and 2.5 V at 100 mA g^{-1}; (b) rate capability test of 25 nm sized SnO_2 hollow sphere; (c) cyclability of SnO_2 hollow spheres with different sizes and commercial SnO_2 nanopowder at 100 mAh g^{-1}.

volume change without a pulverization of electrical pathways. As pointed out in an earlier study [19], the hollow sphere geometry results in less surface area exposed to the electrolyte for an equal volume, which reduces the side reactions and SEI formation and improves the cycle stability.

To confirm the retention of the hollow structure after cycling, the TEM and SEM analyses are conducted on the SnO_2 hollow spheres (Fig. S4, see Electronic Supplementary Material). Compared to the pristine SnO_2 hollow spheres, some deformation (from a circular to an elliptical shape) is observed, but the entire hollow structure is maintained and each hollow sphere is interconnected (Fig. S4b, see Electronic Supplementary Material). The HRTEM image indicates that the shells are composed of nanocrystallites and the shell thickness slightly increases, but a severe grain growth or agglomeration is not observed (Fig. S4c, see Electronic Supplementary Material). The drastic grain growth of SnO_2 or Sn-based material during charge/discharge is the main reason for poor cycle retention, but the current observation indicates that the grain growth is noticeably restricted (Fig. S4d, see Electronic Supplementary Material). Thus, we infer that the hollow nature of the SnO_2 with nano-sized crystallites effectively reduces the grain growth, which results in a high reversible capacity and good cycle retention.

4. Conclusions

In summary, a robust and simple process to fabricate the nano-sized SnO_2 hollow spheres is suggested. The size of SnO_2 hollow spheres is varied from 25 to 100 nm with a constant shell thickness of ~5 nm. Moreover, the size effect of the hollow spheres on the electrochemical properties is demonstrated. The hollow spheres show the stable cycling performance, and the capacity dramatically increases with decreasing the size. The capacity of the smallest SnO_2 hollow sphere is about 750 mAh g^{-1} after 50 cycles and this value approaches the theoretical value of SnO_2. Therefore, it can be concluded that the nano-sized hollow sphere is an ideal structure for the anode material of LIBs.

Acknowledgments

This work was supported by the National Research Foundation of Korea (NRF) grant funded by the Korea government (MEST) (No. 2012-008226).

Appendix A. Supplementary material

Supplementary material associated with this article can be found, in the online version, at http://dx.doi.org/10.1016/j.jpowsour.2012.10.030.

References

[1] Y. Nishi, J. Power Sources 100 (2001) 101–106.
[2] M. Endo, C. Kim, K. Nishimura, T. Fujino, K. Miyashita, Carbon 38 (2000) 183–197.
[3] D. Fauteux, R. Koksbang, J. Appl. Electrochem. 23 (1993) 1–10.
[4] C.-M. Park, J.-H. Kim, H. Kim, H.-J. Sohn, Chem. Soc. Rev. 39 (2010) 3115–3141.
[5] I.A. Courtney, J. Dahn, J. Electrochem. Soc. 144 (1997) 2045.
[6] J. Ye, H. Zhang, R. Yang, X. Li, L. Qi, Small 6 (2010) 296–306.
[7] H. Kim, J. Cho, J. Mater. Chem. 18 (2008) 771–775.
[8] S. Ding, J.S. Chen, G. Qi, X. Duan, Z. Wang, E.P. Giannelis, L.A. Archer, X.W. Lou, J. Am. Chem. Soc. 133 (2010) 21–23.
[9] X.W. Lou, Y. Wang, C. Yuan, J.Y. Lee, L.A. Archer, Adv. Mater. 18 (2006) 2325–2329.
[10] L. Yuan, K. Konstantinov, G.X. Wang, H.K. Liu, S.X. Dou, J. Power Sources 146 (2005) 180–184.
[11] W. Stober, A. Fink, E. Bohn, J. Colloid Interf. Sci. 26 (1968) 62–69.
[12] X.W. Lou, C.M. Li, L.A. Archer, Adv. Mater. 21 (2009) 2536–2539.
[13] X.M. Yin, C.C. Li, M. Zhang, Q.Y. Hao, S. Liu, L.B. Chen, T.H. Wang, J. Phys. Chem. C 114 (2010) 8084–8088.
[14] K.T. Nam, D.-W. Kim, P.J. Yoo, C.-Y. Chiang, N. Meethong, P.T. Hammond, Y.-M. Chiang, A.M. Belcher, Science 312 (2006) 885–888.
[15] J.-M. Tarascon, S. Grugeon, M. Morcrette, S. Laruelle, P. Rozier, P. Poizot, C. R. Chim. 8 (2005) 9–15.
[16] H. Kim, S.-W. Kim, Y.-U. Park, H. Gwon, D.-H. Seo, Y. Kim, K. Kang, Nano Res. 3 (2010) 813–821.
[17] J.S. Chen, C.M. Li, W.W. Zhou, Q.Y. Yan, L.A. Archer, X.W. Lou, Nanoscale 1 (2009) 280–285.
[18] Z. Shan, G. Adesso, A. Cabot, M. Sherburne, S.A.S. Asif, O. Warren, D. Chrzan, A. Minor, A. Alivisatos, Nat. Mater. 7 (2008) 947–952.
[19] Y. Yao, M.T. McDowell, I. Ryu, H. Wu, N. Liu, L. Hu, W.D. Nix, Y. Cui, Nano Lett. 11 (2011) 2949–2954.